

# On the origin of X-ray emission in some FR Is: ADAF or jet?

Qingwen Wu<sup>1,2,3</sup>, Feng Yuan<sup>1,2</sup> and Xinwu Cao<sup>1,2</sup>

## ABSTRACT

We investigate the X-ray origin in FR Is using the radio, submillimetre, optical, and *Chandra* X-ray data of a small sample consisting of eight FR I sources. These sources are very dim, with X-ray luminosities  $L_X/L_{\text{Edd}} \sim 10^{-4} - 10^{-8}$  ( $L_X$  is the X-ray luminosity between 2-10 keV). We try to fit the multiwaveband spectrum using a coupled accretion-jet model. In this model, the accretion flow is described by an advection-dominated accretion flow (ADAF) while in the innermost region of ADAF a fraction of accretion flow is transferred into the vertical direction and forms a jet. We find that X-ray emission in the source with the highest  $L_X$  ( $\sim 1.8 \times 10^{-4} L_{\text{Edd}}$ ) is from the ADAF. The results for the four sources with moderate  $L_X$  ( $\sim \text{several} \times 10^{-6} L_{\text{Edd}}$ ) are complicated. Two are mainly from the ADAFs, one from the jet, and the other from the sum of the jet and ADAF. The X-ray emission in the three least luminous sources ( $L_X \lesssim 1.0 \times 10^{-6} L_{\text{Edd}}$ ) is dominated by the jet although for one source it can also be interpreted by the ADAF since the quality of X-ray data is low. We conclude that these results roughly support the predictions of Yuan & Cui (2005) where they predict that when the X-ray luminosity of the system is below a critical value, the X-radiation will not be dominated by the emission from the ADAF any longer, but by the jet. We also investigate the fuel supply in these sources. We find that the accretion rates in four sources among the five in which we can have good constraints to their accretion rates must be higher than the Bondi rates. This implies that other fuel supply, such as the gas released by the stellar population inside the Bondi radius, should be important.

*Subject headings:* accretion, accretion disks—galaxies: active—galaxies: nuclei—X-rays: galaxies

---

<sup>1</sup>Shanghai Astronomical Observatory, Chinese Academy of Sciences, Shanghai, 200030, China; qwwu@shao.ac.cn, fyuan@shao.ac.cn, cxw@shao.ac.cn

<sup>2</sup>Joint Institute for Galaxy and Cosmology (JOINGC) of SHAO and USMC, 80 Randan Road, Shanghai 200030, China

<sup>3</sup>Graduate School of Chinese Academy of Sciences, Beijing, 100039, China

## 1. Introduction

FR I radio galaxies (defined by edge-darkened radio structure) have lower radio power than FR II galaxies (defined by edge-brightened radio structure due to compact jet terminating hot spots) (Fanaroff & Riley 1974). What causes the morphological difference between FR I and FR II radio galaxies is still unclear. Different explanations of division of FR I and FR II radio galaxies invoke either the interaction of the jet with the ambient medium or the intrinsic nuclei properties of accretion and jet formation processes (e.g., Bicknell 1995; Reynolds et al. 1996a; Gopal-Krishna, & Wiita 2000). Accretion mode in low power FR Is may be different from that in powerful FR IIs. There is growing evidence (Reynolds et al. 1996b; Donato et al. 2004; Gliozzi et al. 2003; Merloni et al. 2003) to suggest that most FR I type radio galaxy nuclei, except for a few 3C FR Is with obscured bright nuclei (Cao & Rawlings 2004), possess advection-dominated accretion flow (ADAF; or “radiative inefficient accretion flows”; Narayan & Yi 1994; 1995; see Narayan, Mahadevan & Quataert 1998 and Kato, Fukue & Mineshige 1998 for reviews). In fact, we now have strong observational evidence that ADAFs may be powering various types of low-luminosity AGNs (LLAGNs; e.g., Fabian & Rees 1995; Reynolds et al. 1996; Quataert et al. 1999; Yuan et al. 2002; Ho, Terashima & Ulvestad 2003; Ptak et al. 2004; Yuan & Narayan 2004; Nemmen et al. 2006; see Narayan 2005, Ho 2005, and Yuan 2007 for reviews) and our Galactic center Sgr A\* (Yuan, Quataert & Narayan 2003; Yuan, Shen & Huang 2006), not only FR Is.

Even so, there are still many details which are unclear and require detailed investigation. One example is the respective contribution of ADAFs and jets at various wavebands in LLAGNs. For FR Is and more general LLAGNs, the least controversial nuclear emission is the radio emission, which is believed to be dominated by the jet (e.g., Wu & Cao 2005). In the optical waveband, *Hubble Space Telescope* (HST) observations show that the optical luminosities of FR Is correlate linearly with their radio nuclear luminosities very well, with little scatter. This, together with the high linear polarization from the nuclear optical emission argues for a synchrotron (jet) origin for the nuclear optical emission (e.g., Chiaberge et al. 1999; Hardcastle et al. 1999). The correlation between the optical nuclear luminosity and radio nuclear luminosity is dual population for FR Is and LINERs (as well as Seyfert). Chiaberge et al. (2005, 2006) suggest that the optical emission of FR Is comes from the jet, while the optical emission of the LINERs and Seyfert is dominated by the accretion flows.

Regarding the X-ray emission, while we usually think that the X-ray emission of LLAGNs comes from the ADAF (e.g., Reynolds et al. 1996b; Quataert et al. 1999), recently it has been proposed that in some individual sources the emission from a jet may be responsible for the observed X-ray emission (e.g., Yuan et al. 2002 for NGC 4258; Fabbiano et al. 2003 for

IC 1459; Pellegrini et al. 2007 for NGC 821; Garcia et al. 2005 for M 31; and references in Yuan & Cui 2005). Then an important question is *systematically* in what kind of condition the radiation from the jet will be important in X-ray band.

There have been several papers toward answering this question. Almost all are based on the correlation between the radio and X-ray luminosities of black hole sources:  $L_R \propto L_X^{0.6}$ , where  $L_R$  is the radio luminosity at 8.6 GHz and  $L_X$  is the 2-11 keV X-ray luminosity. Such a correlation was originally found in the context of the hard state of black hole X-ray binaries (Corbel et al. 2003; Gallo et al. 2003; but see Xue & Cui 2007 and discussion below) and subsequently extended to including LLAGNs as well (Merloni et al. 2003; Falcke et al. 2004; Wang et al. 2006; K rding et al. 2006; Merloni et al. 2006). Such a correlation has sometimes been used to argue in favor of a common origin from the jet (e.g., Markoff et al. 2003; but see Heinz 2004). However, the correlation does not necessarily imply a common jet origin, because it is naturally expected if the mass accretion rate in the ADAF is positively correlated to the mass loss rate in the jet, as is very likely the case. On the other hand, the quantitative result of the correlation does provide us with some important information on the physics of accretion flow and jet and their relation. For example, Merloni et al. (2003) argue that the X-ray emission from low-luminosity black hole sources as used to establish the correlation is most likely dominated by the ADAF rather than a standard thin disk or a jet.

Most sources in Merloni et al. (2003) sample have  $L_X/L_{\text{Edd}} \sim 10^{-7} - 10^{-1}$ . Based on Merloni et al. (2003) correlation result, Yuan & Cui (2005) investigate how the correlation will change at lower luminosities. For this purpose, they first use a coupled ADAF-jet model to explain the observed correlation (within the range of  $L_X/L_{\text{Edd}} \sim 10^{-7} - 10^{-1}$ ). The X-ray emission is modeled by thermal Comptonization emission in the ADAF, while the radio emission is modeled as due to the synchrotron emission in the jet. To quantitatively explain the correlation, they find that the ratio of the mass loss rate in the jet to the mass accretion rate in the ADAF,  $\dot{M}_{\text{jet}}/\dot{M}$ , is not, but not far away from, a constant with the changing  $\dot{M}$ . Extrapolating this ratio to lower  $\dot{M}$  or  $L_X$  ( $< 10^{-7}L_{\text{Edd}}$ ) and assuming that the physics of jet remain unchanged at the same time, they find that the X-ray emission of the system should be dominated by the jet when  $L_X$  is lower than a critical value  $L_{X,\text{crit}}$  determined by

$$\log \left( \frac{L_{X,\text{crit}}}{L_{\text{Edd}}} \right) = -5.356 - 0.17 \log \left( \frac{\dot{M}}{\dot{M}_{\odot}} \right) \quad (1)$$

The physical reason is that with the decrease of the accretion rate, both the X-ray radiation from the ADAF and the jet will decrease. The former decreases faster since it is roughly proportional to  $\dot{M}^2$  while the latter to  $\dot{M}$ . Below a certain  $\dot{M}$  which corresponds to  $L_{X,\text{crit}}$ , the X-ray emission from the jet will dominate over the ADAF. In this low  $\dot{M}$  regime, both

the radio and X-ray emissions are from the jet, thus the radio-X-ray correlation will change, with the correlation index changing from  $\sim 0.6$  to  $\sim 1.2$  (see also Heinz 2004). We want to emphasize that the normalization of the correlation adopted in Yuan & Cui (2005) is based on the data of XTE J1118+480. Because of the large scatter of the correlation (ref. Merloni et al. 2003), and because of the statistical feature of the correlation, for individual sources, the exact value of  $L_{X,\text{crit}}$  could be significantly different from that estimated in eq. (1). The prediction thus only has statistical meaning.

Similar to Yuan & Cui (2005), Fender et al. (2003) also pointed out the important role of jets when the X-ray luminosity of the system,  $L_X$ , is very low. They compared the power of the jets,  $P_{\text{jet}}$ , and  $L_X$ . They found that when  $L_X$  is lower than a critical value,  $P_{\text{jet}}$  is larger than  $L_X$ . The difference between this work and Yuan & Cui (2005) is that the former compared  $L_X$  with the *total power of the jet*  $P_{\text{jet}}$  rather than the *emitted X-ray luminosity* from the jet.

The main aim of the present paper is to check the prediction of Yuan & Cui (2005). For this purpose we select a small sample of Donato et al. (2004) since  $L_X/L_{\text{Edd}}$  ranges from  $\sim 10^{-4}$  to  $\sim 10^{-8}$ . We want to check whether the dominance of X-ray emission will change from an ADAF to a jet when the luminosity decreases.

Another reason we choose this sample is that we want to investigate the question of fuel supply. Observationally we have good estimation to the Bondi accretion rate in all the sources in this sample. On the other hand, when the X-ray spectrum comes from the ADAF, we can obtain the required value of mass accretion rate based on the accretion disk model. We thus can investigate how good the Bondi accretion rate is as an indicator of the accretion rate.

In §2 and §3, we introduce the sample and the coupled ADAF-jet model respectively. The modeling results are presented in §4, and the discussion and summary are presented in §5 & 6. Throughout this paper, we adopt  $H_0 = 70 \text{ km s}^{-1} \text{ Mpc}^{-1}$ ,  $\Omega_M = 0.3$ , and  $\Omega_\Lambda = 0.7$ .

## 2. Sample

The FR I sample used for the present investigation is selected from Donato et al. (2004). The sources in this sample have estimated black hole mass, Bondi accretion rate, optical, radio, and X-ray nuclear emission. There are 9 FR Is in their sample which have compact core X-ray emission and have been observed by *Chandra*. We excluded 3C 270 since the optical emission may be obscured by its large intrinsic column density ( $N_H \sim 10^{22} \text{ cm}^{-2}$ ). Therefore, our final sample include 8 FR Is (see Donato et al. 2004, for more details). We have com-

piled in Table 1 the nuclear luminosity obtained from literature in the radio, submillimetre, infrared, optical, ultraviolet(UV) and X-ray bands. This sample is ideal for us to check the prediction of Yuan & Cui (2005), since the range of X-ray luminosities is  $\sim (10^{-4} - 10^{-8})L_{\text{Edd}}$

### 3. Coupled accretion-jet model

We briefly describe the ADAF-jet model here. The readers can refer to Yuan, Cui & Narayan (2005) for the details. The accretion flow is described by an ADAF. In past few years, both numerical simulations (Stone, Pringle, & Begelman 1999; Hawley & Balbus 2002; Igumenshchev et al. 2003) and analytical work (Narayan & Yi 1994, 1995; Blandford & Begelman 1999; Narayan et al. 2000; Quataert & Gruzinov 2000) indicate that probably only a fraction of the gas that is available at large radius actually accretes onto the black hole. The rest of the gas is either ejected from the flow or is prevented from being accreted by convective motions. Following the proposal due to Blandford & Begelman (1999), we can parameterize the radial variation of the accretion rate with the parameter  $p_w$ ,  $\dot{M} = \dot{M}_{\text{out}}(R/R_{\text{out}})^{p_w}$ , where  $\dot{M}_{\text{out}}$  is the accretion rate at the outer boundary of the ADAF  $R_{\text{out}}$ . We calculate the global solution of the ADAF. The viscosity parameter  $\alpha$  and magnetic parameter  $\beta$  (defined as ratio of gas to total pressure in the accretion flow,  $\beta = P_g/P_{\text{tot}}$ ) are fixed to be  $\alpha = 0.3$  and  $\beta = 0.9$ . Another parameter is  $\delta$ , describing the fraction of the turbulent dissipation which directly heats electrons. Following Yuan et al. (2006), we use  $\delta = 0.3$  and  $p_w = 0.25$  in all our calculations.

The radiative processes we consider include synchrotron, bremsstrahlung and their Comptonization. We set the outer boundary of the ADAF at the Bondi radius  $R_B = 2GM_{\text{BH}}/c_s^2$ ,  $c_s = \sqrt{\gamma kT/\mu m_p}$  is the adiabatic sound speed of the gas at the Bondi accretion radius,  $T$  is the gas temperature at that radius,  $\mu = 0.62$  is the mean atomic weight,  $m_p$  is the proton mass and  $\gamma = 4/3$  is adiabatic index of the X-ray emitting gas. After the ADAF structure is obtained, the spectrum of the flow can be calculated(e.g., Yuan, Quataert & Narayan 2003).

The jet model adopted in the present paper is based on the internal shock scenario, widely used in interpreting gamma-ray burst (GRB) afterglows (see, Spada et al. 2001; Piran 1999). A fraction of the material in the accretion flow is assumed to be transferred into the vertical direction to form a jet. The jet is assumed to include equal numbers of protons and electrons. Since the velocity of the accretion flow is supersonic near the black hole(BH), a standing shock should occur at the bottom of the jet because of bending. From the shock jump conditions, we calculate the properties of the postshock flow, such as electron temperature  $T_e$ . The jet is assumed to have a conical geometry with half-open angle  $\phi$  and

bulk Lorentz factor  $\Gamma_j$  which are independent of the distance from the BH. The internal shock in the jet should occur as a result of the collision of shells with different  $\Gamma_j$ , and these shocks accelerate a small fraction of the electrons into power-law energy distribution with index  $p$ . We assume that the fraction of accelerated electrons in the shock is  $\xi_e$  and fix  $\xi_e = 10\%$  in our calculations. Following the widely adopted approach in the study of GRBs, the energy density of accelerated electrons and amplified magnetic field are described by two free parameters  $\epsilon_e$  and  $\epsilon_B$ . Obviously,  $\xi_e$  and  $\epsilon_e$  are not independent. The half-open angle of the conical jet is assumed to be  $\phi = 0.1$ , which is the typical value for the inner jet in FR Is and does not affect our results (e.g., Laing & Bridle 2002). We find that the Lorentz factor has only a modest effect on the best fit of the jet spectrum if it is in the typical range  $\Gamma_j \sim 2 - 5$  (or  $v/c \sim 0.9$ ) of FR Is (e.g., Verdoes Kleijn et al. 2002; Laing & Bridle 2002; Bondi et al. 2000). Laing et al. (1999) also concluded that the typical on-axis velocity of the inner jet was  $v/c \sim 0.9$  for FR Is. For simplicity, we set the  $\Gamma_j = 2.3$  (corresponding to  $v/c = 0.9$ ) in jet spectra calculations if there is no estimation on the Lorentz factor.

We consider only synchrotron emission in jet spectrum calculation, since Compton scattering is probably not important in these FR Is for several reasons. Firstly, our calculation show that the synchrotron self-Compton (SSC) in the jet is several magnitude less than the synchrotron emission in these FR Is since the ratio of the photon energy density to the magnetic field energy density is very low (thin long-dashed lines in Figures in this paper). Secondly, Compton scattering of the external photons from the disk and emission lines should also not be important because the disk emission is rather low, and there may be a lack of broad emission lines in FR Is (e.g., Chiaberge et al. 1999). Thirdly, the inverse Compton scattering of cosmic microwave radiation should be unimportant for these FR Is since this mechanism requires high-velocity bulk motion of the jet, which may be present only in powerful FR II radio galaxies (e.g., Celotti et al. 2001).

We treat the mass loss rate into the jet,  $\dot{M}_{\text{jet}}$ , and accretion rate in the accretion flow,  $\dot{M}_{\text{out}}$ , as free parameters when fitting the spectrum, since the jet formation mechanism is still unclear. The other free parameters in spectral fitting are the electron energy spectral index,  $p$ , the electron/magnetic energy parameter,  $\epsilon_e$ ,  $\epsilon_B$ . We use dimensionless accretion rate  $\dot{m} = \dot{M}/\dot{M}_{\text{Edd}}$  throughout the paper. The consistency between the ADAF and jet models will be ensured by checking whether the value of  $\dot{M}_{\text{jet}}/\dot{M}_{\text{out}}$ , or more precisely  $\dot{M}_{\text{jet}}/\dot{M}(10R_s)$  (see next section), is reasonable.

## 4. Spectral fitting results

We use the ADAF-jet model to fit the spectrum of the sources in our sample. As we state in §1, the radio emission, and perhaps optical as well, is from the jet. Although the jet model is more uncertain than the ADAF, based on the assumption to the jet model described in §3, the contribution of the jet to the X-ray band is well constrained once we require the jet to explain the radio and optical spectrum. We then adjust the parameter of the ADAF and combine it with the jet contribution to fit the X-ray spectrum.

### 4.1. 3C 346

The radio morphology and power of 3C 346 would rank it as either a low-power FR II source or a high-power FR I (e.g., Spencer et al. 1991). Cotton et al. (1995) used the Very Long Baseline Interferometry (VLBI) radio core dominance and jet to counter jet ratio to argue for a viewing angle of the jet is about  $< 32^\circ$  and a speed of  $> 0.8c$ . *Chandra* observation have detected an unresolved core with 2-10 keV luminosity of  $1.9 \times 10^{43}$  erg s $^{-1}$  and photon index of  $\Gamma = 1.69^{+0.09}_{-0.09}$  (Donato et al. 2004). An X-ray knot is also detected by *Chandra* with a photon index  $\Gamma = 2.0 \pm 0.3$  and no intrinsic absorption, which roughly corresponding to the brightest radio and optical knot (Worrall & Birkinshaw 2005).

Figure 1 shows the fitting result. The dashed, dot-dashed, and the solid lines show the emission of the jet, ADAF, and their sum respectively. The parameters of the jet are  $\dot{m}_{\text{jet}} = 3.5 \times 10^{-5}$ ,  $\epsilon_e = 0.14$ ,  $\epsilon_B = 0.02$ , and  $p = 2.4$ . We find that the jet model can describe well the nuclear radio and optical emission. But the X-ray emission of the jet model is several times lower than the *Chandra* observations. The X-ray emission can be well fitted by the underlying ADAF. The required accretion rate is  $\dot{m}_{\text{out}} = 2.8 \times 10^{-2}$ . The ratio of mass loss rate in the jet to accretion rate of ADAF at  $10 R_S$  is about  $\dot{m}_{\text{jet}}/\dot{m}(10R_S) = 0.9\%$ , where  $R_S$  is Schwarzschild radius.

This source is relatively luminous, with  $L_X/L_{\text{Edd}} = 1.8 \times 10^{-4}$ . The X-ray luminosity is well above the critical luminosity defined in eq. (1). Thus according to Yuan & Cui (2005), the X-ray emission should be dominated by the ADAF rather than the jet. Our modeling result confirms this prediction.

#### 4.2. B2 0755+37

B2 0755+37 is a well studied nearby FR I ( $z = 0.0428$ ) with two large symmetrical lobes and very asymmetric jets. The inferred velocity of the jet is  $\sim 0.9c$  (1 arcsec from the core,  $\sim 0.5$  kpc), and the viewing angle is about  $30^\circ$  (Bondi et al. 2000). In the optical band, the galaxy has a rather smooth appearance without any sign of dust obscuration, and a bright optical nucleus is seen at its center (Capetti et al. 2002). The optical jet is also detected, and the optical brightness profile is similar to that of radio (Parma et al. 2003). A power-law fit to the nuclear emission observed by *Chandra* results in a power-law index  $\Gamma = 2.18^{+0.28}_{-0.19}$  and 2-10 keV luminosity of  $6.1 \times 10^{41}$  erg s $^{-1}$  ( $\sim 5.2 \times 10^{-6} L_{\text{Edd}}$ ) (Donato et al. 2004).

Figure 2 shows the fitting result of B2 0755+37. The dashed-line shows the jet emission. The parameters are  $\dot{m}_{\text{jet}} = 1.75 \times 10^{-5}$ ,  $\epsilon_e = 0.12$ ,  $\epsilon_B = 0.01$ , and  $p = 2.23$ . We find that the jet model can not only well describe the radio and optical spectra, but also X-ray spectrum.

The dot-dashed line shows the emission from an ADAF model, with  $\dot{m}_{\text{out}} = 8.9 \times 10^{-3}$ . This is of course not a ‘fit’. We show this result to illustrate that an ADAF would predict a much harder X-ray spectrum than observed. This is another evidence for the dominance of the X-ray emission by the jet. Obviously  $\dot{m}_{\text{out}}$  should be the upper limit of accretion rate.

#### 4.3. 3C 31

3C 31 is also a twin-jet FR I radio galaxy (redshift  $z=0.0169$ ), hosted by the D galaxy NGC 383. 3C 31 has been widely studied in the radio, optical and X-ray bands (e.g., Martel et al. 2000; Laing & Bridle 2002; Hardcastle et al. 2002). High quality radio imaging with Very Large Array (VLA) allowed Laing & Bridle (2002) to make detailed models of velocity field in the jets within 30 arcsec of the nucleus, on the assumption that the jets are intrinsically symmetrical and anti-parallel. They inferred the angle to the line of sight to be  $52^\circ$  with an uncertainty of a few degrees, and found that central velocity is  $\sim 0.87c$  for the inner region (0 to 1.1 kpc). The *HST* image reveals a nearly face-on dust disk surrounding the unresolved galaxy’s nucleus (e.g., Martel et al. 1999). From the *Chandra* observation of November 2000, the inner region has been resolved in the point-like X-ray core and an extended X-ray jet (Hardcastle et al. 2002). The spectrum of the core is quite flat, with photon index  $\Gamma = 1.48^{+0.28}_{-0.32}$  and the 2-10 keV nuclear X-ray luminosity is  $4.7 \times 10^{40}$  erg s $^{-1}$  ( $\sim 4.4 \times 10^{-6} L_{\text{Edd}}$ ) (Evans et al. 2006). The X-ray jet can be fitted by a power-law model with a photon index  $\Gamma = 2.09 \pm 0.16$  (Hardcastle et al. 2002).

Figure 3 shows the fitting result of 3C 31. The dashed and dot-dashed lines are for the emissions from the jet and the ADAF, respectively, and the solid line shows their sum. The



parameters of the jet are  $\dot{m}_{\text{jet}} = 2.7 \times 10^{-5}$ ,  $\epsilon_e = 0.2$ ,  $\epsilon_B = 0.02$ , and  $p = 2.5$ . We find that the radio, optical and even the soft X-ray nuclear emission (e.g., 1 keV) can be well fitted by a pure jet model. However, the hard X-ray cannot be fitted by a jet, but can be well fitted by the underlying ADAF with accretion rate  $\dot{m}_{\text{out}} = 3.7 \times 10^{-3}$ . The ratio,  $\dot{m}_{\text{jet}}/\dot{m}(10 R_S)$ , is about 9%.

#### 4.4. 3C 317

The radio galaxy 3C 317 is associated with CD galaxy UGC 9799 ( $z = 0.0345$ ), located at the centre of the cooling flow cluster A 2052. The radio observation shows that it may be a very young radio source (Venturi et al. 2004). Unresolved compact core is observed by *HST* in both optical and UV band. However, the core emission show strong variability in the UV band between 1994 and 1999 (by a factor of 10, Chiaberge et al. 2002). The spectral index of optical-UV is very large,  $\alpha_{\text{opt-UV}} = 3.3$  ( $F_\nu \propto \nu^{-\alpha}$ , Chiaberge et al. 2002). The central compact core is also detected by *Chandra* with 2-10 keV power-law luminosity  $2.97 \times 10^{41} \text{ erg s}^{-1}$  ( $\sim 3.4 \times 10^{-6} L_{\text{Edd}}$ ) and a photon index  $\Gamma = 1.81_{-0.1}^{+0.13}$  (Donato et al. 2004).

Figure 4 shows the fitting result of 3C 317. The dashed, dot-dashed lines show the emissions from the jet and ADAF respectively, while the solid line shows their sum. The parameters of the jet are  $\dot{m}_{\text{jet}} = 1.7 \times 10^{-5}$ ,  $\epsilon_e = 0.2$ ,  $\epsilon_B = 0.15$ , and  $p = 2.25$ . It is difficult to fit the radio and optical emission simultaneously due to the steep optical-UV spectrum. Since the UV flux is very sensitive to the extinction, such a steep spectrum may be not intrinsic. We therefore use *R* band (F702W) in our fits, which is less susceptible to extinction than the UV band and less contaminated by the possible dust emission than the near-infrared band (*H* band, F160W). The radio, optical and even soft X-ray band (e.g., 1 keV) emission can be fitted by a jet model. The hard X-ray spectrum can not be well fitted by the pure jet or underlying ADAF alone. Rather, it can be well fitted by their sum. The required accretion rate of the ADAF is  $\dot{m}_{\text{out}} = 4.7 \times 10^{-3}$ .

#### 4.5. B2 0055+30

The source B2 0055+30 (NGC 315) is associated with a giant elliptical galaxy at a redshift of 0.0168, which has a two-side structure extending to roughly one degree on the sky (Bridle et al. 1979). Canvin et al. (2005) applied symmetrical, deceleration, relativistic jet model to fit the radio jet, and derived the inclination to the line of sight of  $38^\circ \pm 2^\circ$  and their on-axis velocity is  $\beta = v/c \sim 0.9$ . The jet is also detected by *Chandra* with a power

law index  $\Gamma = 1.5 \pm 0.7$  (Worrall et al. 2003). The 2-10 keV nuclear luminosity detected by *Chandra* is  $5.1 \times 10^{41} \text{ erg s}^{-1}$  ( $\sim 2.4 \times 10^{-6} L_{\text{Edd}}$ ) with a photon index  $\Gamma = 1.56_{-0.09}^{+0.17}$  (Donato et al. 2004).

Figure 5 shows the fitting result of B2 0055+30. The dashed and dot-dashed lines show the emissions from the jet and ADAF respectively, while the solid line shows their sum. The parameters of the jet are  $\dot{m}_{\text{jet}} = 7.0 \times 10^{-6}$ ,  $\epsilon_e = 0.05$ ,  $\epsilon_B = 0.02$ , and  $p = 2.2$ . We can see from the figure that the radio and optical emission can be well fitted by the jet model. However, the X-ray spectrum is too hard to be fitted by the jet, but can be well fitted by the ADAF with the accretion rate  $\dot{m}_{\text{out}} = 2.7 \times 10^{-3}$ . The ratio  $\dot{m}_{\text{jet}}/\dot{m}(10 R_S)$  is about 3.5%.

#### 4.6. 3C 66B

3C 66B has a redshift of 0.0212 and is associated with a thirteen-magnitude elliptical galaxy in a small group in the vicinity of the cluster Abell 347. The two-sided inner radio jets is seen, with both jets curving toward the east at distance  $> 20'' - 30''$  from the core (Leahy et al. 1986). *HST* observed the optical jet on scales of  $\sim 0.1$  arcsec (Macchetto et al. 1991). The jet also been imaged with *Infrared Space Observatory (ISO)* and *Chandra* (Tansley et al. 2000; Hardcastle et al. 2001). The multi-wavelength extended jet emission can be well fitted with the synchrotron emission (e.g., Tansley et al. 2000). The point-like nucleus is detected by *Chandra* with 2-10 keV luminosity  $1.1 \times 10^{41} \text{ ergs}^{-1}$  ( $\sim 1 \times 10^{-6} L_{\text{Edd}}$ ) and a photon index  $\Gamma = 2.17_{-0.15}^{+0.14}$  (e.g., Donato et al. 2004).

Figure 6 shows the fitting result of nucleus of 3C 66B. We find that both the radio, submillimetre, optical and X-ray can be fitted by pure jet model very well (dashed line). The parameters of the jet are  $\dot{m}_{\text{jet}} = 1 \times 10^{-5}$ ,  $\epsilon_e = 0.18$ ,  $\epsilon_B = 0.02$ , and  $p = 2.35$ . For illustration purpose, we also show by the dot-dashed line the X-ray emission using an ADAF model with  $\dot{m}_{\text{out}} = 2.6 \times 10^{-3}$ . We can see that the predicted spectrum by an ADAF is too hard to be consistent with the observation (so the accretion rate in the ADAF should be smaller than  $2.6 \times 10^{-3}$ ). The X-ray emission in this source should be from the jet.

#### 4.7. 3C 449

3C 449 is a low-redshift ( $z=0.0171$ ) twin-jet FR I type radio galaxy which hosted by the elliptical galaxy UGC 12064. Its symmetrical inner jets have been well studied in the radio observation (e.g., Feretti et al. 1999). On large scales, the southern jet flares into a lobe, while the northern jet continue to be well collimated until it fades into the noise (e.g.,

Andernach et al. 1992; Feretti et al. 1999). From the application of the adiabatic model to the jet, evidence of a strong jet deceleration within  $10''$  (5 kpc) from the nucleus is found. A satisfactory fit to the data is found assuming an initial jet velocity  $0.9c$ , and a jet inclination to the line of sight of  $82.5^\circ$  (e.g., Feretti et al. 1999). The nucleus is an unresolved point source from *HST* observation (e.g., Martel et al. 1999). *Chandra* observation exhibit a X-ray central compact core with a power-law photon index  $\Gamma = 1.67^{+0.45}_{-0.49}$  and the 2-10 keV power-law luminosity is less than  $2.9 \times 10^{40} \text{ erg s}^{-1}$  ( $\sim 8 \times 10^{-7} L_{\text{Edd}}$ ) (Evans et al. 2006). Evans et al. (2006) shown that the X-ray luminosity observed by *Chandra* is several times lower than that measured by *XMM-Newton* and it's photon index is also flatter than  $\Gamma = 2.13^{+0.65}_{-0.55}$  of *XMM-Newton* (Donato et al. 2004). Although the variability is a possible explanation for the difference observed by *Chandra* and *XMM-Newton*, it may be also due to the different resolution of the telescopes. The spectrum is extracted in a smaller radius circle (typically 2.5 pixels or  $1''.23$  in the case of *Chandra*) than  $35''$  in the case of *XMM-Newton* (Evans et al. 2006). *Chandra* observation should reflect the intrinsic nuclear X-ray emission, while *XMM-Newton* observation may be contaminated by the X-ray jet emission and/or X-ray binaries.

Figure 7 shows the fitting result of 3C 449. We find that the radio, optical and X-ray emissions can be roughly fitted by a pure jet model shown by the thick long-dashed line. The parameters are  $\dot{m}_{\text{jet}} = 4.0 \times 10^{-5}$ ,  $\epsilon_e = 0.45$ ,  $\epsilon_B = 0.003$ , and  $p = 2.25$ .

Since the observational error in the X-ray photon index is very large, we also try to fit the X-ray emission with the sum of a jet and an ADAF. The thin short-dashed and dot-dashed lines show the emissions from the jet and the ADAF respectively and the solid line shows their sum. The parameters of the jet are  $\dot{m}_{\text{jet}} = 2.0 \times 10^{-5}$ ,  $\epsilon_e = 0.35$ ,  $\epsilon_B = 0.01$ , and  $p = 2.4$ . The accretion rate of the ADAF is  $\dot{m}_{\text{out}} = 1.9 \times 10^{-3}$ . We can see that the X-ray emission can also be (slightly better because of more free parameters) fitted by the sum of ADAF and jet. The value of  $\dot{m}_{\text{jet}}/\dot{m}(10 R_s)$  is about 14.3%. Higher quality X-ray data is desired to further constrain the origin of the X-ray emission in 3C 449.

#### 4.8. 3C 272.1

3C 272.1 (M 84=NGC 4374) is an E1 galaxy in the core of the Virgo Cluster ( $z=0.0029$ ). Radio observations at 1.4 and 4.9 GHz show two lobes and a jet (Laing & Bridle 1987). In the SCUBA 850- $\mu\text{m}$  submillimetre image, the galaxy is found to be a point source (diameter  $<15$  arcsec, 1.5kpc). The submillimetre emission was suggested to be from the inner jet, or from the emission from the thermal emission of cold diffuse dust (Leeuw et al. 2000). *HST* show that the optical-to-UV continuum is very red, similar to the spectral energy distribution

of BL Lac (Bower et al. 2000). The *Chandra* image show that the soft X-ray emission have a very disturbed morphology. Donato et al. (2004) defined this source as a candidate compact core X-ray source, since that its radial profile cannot be fitted with a  $\beta$ -model. The 2-10 keV luminosity is  $2.2 \times 10^{39} \text{ergs}^{-1}$  ( $\sim 6.8 \times 10^{-8} L_{\text{Edd}}$ ) with a photon index  $\Gamma = 2.14_{-0.30}^{+0.34}$  (Evans et al. 2006).

Figure 8 shows the fitting result of nucleus of 3C 272.1. The dashed and the dot-dashed lines show the emissions from the jet and the ADAF respectively. The parameters of the jet are  $\dot{m}_{\text{jet}} = 4.9 \times 10^{-6}$ ,  $\epsilon_e = 0.28$ ,  $\epsilon_B = 0.005$ , and  $p = 2.5$ . We can see that the radio, submillimetre, optical and especially X-ray emission can be fitted by the jet model very well. On the other hand, the predicted spectrum by an ADAF (with  $\dot{m}_{\text{out}} = 1.9 \times 10^{-3}$ ) is too hard to be consistent with observation. So in this source, the X-ray emission is dominated by a jet.

## 5. Discussion

In this paper we have investigated the origin of the X-ray emission in a small sample from FR Is in Donato et al. (2004). The accretion flow in FR Is is generally believed to be described by an ADAF rather than a standard thin disk since the Bondi accretion rates (which should be a lower limit, see discussion below) would produce a luminosity several orders of magnitude higher than that observed if we assume a standard thin disk with the efficiency of  $\sim 0.1$  as in a standard thin disk. Two possibilities exist for the X-ray origin in FR Is–ADAF or jet. We use a coupled ADAF-jet model to fit the multiwaveband spectrum to try to investigate this problem. More specifically, we want to examine the prediction of Yuan & Cui (2005) that statistically the X-ray emission in LLAGNs should be dominated by ADAFs when their X-ray luminosity is higher than  $\sim \text{a few} \times 10^{-7} L_{\text{Edd}}$ , but will be dominated by jet when the luminosity is lower than this value.

We find that the jet can well describe the radio and optical spectra for all FR Is in our sample except the optical/UV spectrum in 3C 317 (see our argument on this point in §4.4). The soft X-ray flux at  $\sim 1$  keV of all FR Is is roughly consistent with the predictions of the jet. This result indicates why a tight correlation is found among radio, optical and soft X-ray (e.g., Chiaberge et al. 1999; Evans et al. 2006; Balmaverde et al. 2006).

For the source with the highest luminosity in our sample, 3C 346, which has  $L_X = 1.8 \times 10^{-4} L_{\text{Edd}}$ , its X-ray spectrum is dominated by the ADAF and the jet contribution is negligible. However, for the four sources with “intermediate luminosities” (B2 0755+37, 3C 31, 3C 317, B2 0055+30;  $L_X = (2.4 - 5.2) \times 10^{-6} L_{\text{Edd}}$ ), their X-ray origin is complicated. The

X-ray spectra of B2 0755+37 is dominated by the jet while for 3C 31 and B2 0055+30 they are dominated by the ADAF. For the other one (3C 317), the contributions of the ADAF and jet are comparable. For the three least luminous sources (3C 66B, 3C 449 and 3C 272.1) which have  $L_X = (6.8 \times 10^{-8} - 1 \times 10^{-6})L_{\text{Edd}}$ , their X-ray spectra are dominated by the jet. The X-ray emission of 3C 449 is also interpreted by the sum of a jet and an ADAF, which requires higher quality data to further constrain it.

Our results are roughly consistent with the predictions of Yuan & Cui (2005). The “intermediate luminosity” here in our sample corresponds to the critical luminosity in Yuan & Cui (2005). However, the former is about 10 times higher than the latter. The value of the critical luminosity depends on the ratio of the mass loss rate in the jet to the mass accretion rate in the ADAF. This ratio is adopted in Yuan & Cui (2005) from fitting the data of a black hole X-ray binary—XTE J1118+480. The current result indicates that the ratio in FR Is is about 10 times higher than in XTE J1118+480. This seems reasonable given that the jet in FR Is is systematically more powerful than in normal LLAGNs. One possible reason could be that systematically the black holes in FR Is are spinning more rapidly.

The sample we used in the present paper is rather small. Obviously to systematically study the X-ray origin of FR Is and more generally LLAGNs a much larger sample is required and this is our future work (Yuan et al. in preparation). We note that current results from literature seem to support the prediction of Yuan & Cui (2005). In addition to the observational evidences listed in Yuan & Cui (2005), the X-ray emission of some LLAGNs claimed to be dominated by jet always have  $L_X < L_{X,\text{crit}} \sim (10^{-6} - 10^{-7})L_{\text{Edd}}$ —NGC 821:  $L_X/L_{\text{Edd}} \sim 3.0 \times 10^{-7}$  (Fabbiano et al. 2004); IC 1459:  $L_X/L_{\text{Edd}} \sim 2.9 \times 10^{-7}$  (Fabbiano et al. 2003); NGC 4594:  $L_X/L_{\text{Edd}} \sim 1.0 \times 10^{-7}$  (Pellegrini et al. 2003); M 31:  $L_X/L_{\text{Edd}} \sim 2.2 \times 10^{-10}$  (Garcia et al. 2005). On the other hand, the ADAF contribution usually dominates over jet for the sources with  $L_X > L_{X,\text{crit}}$ —NGC 4261:  $L_X/L_{\text{Edd}} \sim 1.4 \times 10^{-6}$  (Gliozzi et al. 2003); NGC 3998:  $L_X/L_{\text{Edd}} \sim 2.0 \times 10^{-6}$  (Ptak et al. 2004). Another interesting result we would like to mention is the correlation between  $\dot{m}(10R_s)$  and  $\dot{m}_{\text{jet}}/\dot{m}(10R_s)$ , i.e., columns 7 & 8 in Table 2. We can find that the sources with the highest  $\dot{m}(10R_s)$  have the smallest  $\dot{m}_{\text{jet}}/\dot{m}(10R_s)$  (3C 346), and lower  $\dot{m}(10R_s)$  sources have larger  $\dot{m}_{\text{jet}}/\dot{m}(10R_s)$ . This result is roughly consistent with the prediction of Yuan & Cui 2005 (their Fig. 2). But we want to emphasize again that a larger sample is required to more seriously check this prediction.

As we emphasize earlier, the radio-X-ray correlation and therefore the prediction of Yuan & Cui (2005) only holds in statistical sense and may not be valid for any individual source. In fact, a most recent critical examination of the radio/X-ray data in a sample of black hole X-ray binaries has shown that the correlation is very diverse and some sources don’t show such a correlation (Xue & Cui 2007; see also Rodriguez et al. 2007). Recently

Gallo et al. (2006) obtain one radio/X-ray data set in the quiescent state of A0620-00, with  $L_X \sim 10^{-8.5} L_{\text{Edd}} \ll L_{X,\text{crit}}$ . They find that the data lies on the extrapolation of the radio-X-ray correlation, without change of the correlation index. Thus A0620-00 may be another exception. On the other hand, however, we would like to point out a caveat in Gallo et al. (2006). Given the very large scatter in the radio-X-ray correlation (Merloni et al. 2003; Gallo et al. 2003), it is not appropriate to connect one data point of *a source* with the data of *other different* sources because their normalization may be different. Rather, one should combine the radio and X-ray data at different luminosities only for A0620-00. Although we do have X-ray and radio observations during its 1975 outburst (Kuulkers 1998), we are unfortunately not able to convert the X-ray “counts” to physical flux due to instrumental reasons.

Typically Bondi accretion rate is a good estimation to the mass accretion rate. However, Pellegrini (2005) show that there is no relation between the nuclear X-ray luminosity and Bondi accretion rate in LLAGNs, and X-ray emission of some sources is higher than the values predicted by ADAFs with Bondi accretion rate. In this paper, the Bondi accretion rate in our sample have been estimated (Donato et al. 2004). We find that the accretion rates  $\dot{m}_{\text{out}}$  required in our model of four FR Is (3C 346, 3C 31, 3C 449, 3C 317) among the five in which we can have good constraints to their accretion rates are higher than their Bondi rates by factors of 9, 18, 112<sup>1</sup>, 1.05, respectively. Given that the radial velocity of the accretion flow is  $\alpha c_s$ , a more accurate estimation of the accretion rate is  $\dot{m}_{\text{out}} \sim \alpha \dot{m}_{\text{Bondi}}$  where  $\alpha$  is the viscous parameter (Narayan 2002). Therefore the Bondi accretion rate is only a lower limit of the real rate and other fuel supply must be important, such as the gas released by the stellar population inside the Bondi radius (Soria et al. 2006; Pellegrini 2007). In our calculation, given the theoretical uncertainties about the values of  $p_w$  and  $\delta$ , we choose the values of these two parameters from the best studied source, Sgr A\* (Yuan et al. 2006; Yuan, Quataert & Narayan 2003), because we think the physics of accretion should be the same, independent of various sources. A higher  $\delta$  and lower  $p_w$  incline to require a smaller accretion rate. But we find that even though we use  $\delta = 0.5$ , which mean half of the viscous dissipation directly heats electrons, and  $p_w = 0$ , which mean no outflow, the required accretion rates for 3C 346, 3C 31, and 3C 449 are still larger than their Bondi accretion rates. Therefore, other fuel supply must be important in these sources.

The kinetic luminosity,  $L_{\text{kin}} = \Gamma_j(\Gamma_j - 1)\dot{M}_{\text{jet}}c^2$ , can be derived from our modeling results. We use  $\eta_{\text{jet}} = L_{\text{kin}}/\dot{M}(10R_S)c^2$  to describe the efficiency of the jet power converted from the accretion power, where  $\dot{M}(10R_S)$  is mass accretion rate at  $10R_S$ . We find that

---

<sup>1</sup>The accretion rate of 3C 449 is calculated from the X-ray emission based on the ADAF model, which should be the upper limit if the X-ray emission is dominated by the jet as discussed in §4.7 and §5.

$\eta_{\text{jet}} = 0.03 - 0.44$  for the sources in this sample (see Table 2), and most of them (six of eight) have  $\eta_{\text{jet}}$  significantly higher than 0.057 which is the largest available accretion energy at the innermost stable circular orbit (ISCO) for a nonrotating black hole. This either imply that the black holes in these sources are spinning rapidly (so ISCO is smaller thus more accretion energy is available, or the jet power is extracted from the spinning black holes via the BZ process; Blandford & Znajek 1977; Reynolds et al. 2006), or the accretion energy within ISCO can be extracted through magnetic field. We have assumed that the jet includes equal numbers of protons and electrons. If the jet is enhanced by pairs, it could give the same emission but with much less kinetic luminosity and less BH spins.

## 6. Summary

We have fitted the multiwaveband spectra of 8 FR Is ranging from radio to X-ray with our coupled ADAF-jet model. We find that the origin of X-ray emission can be from ADAF, jet, or their sum, depending on the ratio of  $L_X/L_{\text{Edd}}$ , here  $L_X$  is the X-ray luminosity. When  $L_X$  is significantly larger than a critical value  $L_{X,\text{crit}}$ , the X-ray emission will be dominated by an ADAF. When  $L_X$  is significantly smaller than  $L_{X,\text{crit}}$ , it will be dominated by a jet. The contributions of the ADAFs and jets are capable when  $L_X \sim L_{X,\text{crit}}$ . These results roughly support the prediction of Yuan & Cui (2005), except that the value of  $L_{X,\text{crit}}$  here, several times of  $10^{-6}L_{\text{Edd}}$ , is  $\sim 10$  times higher than the predicted value in Yuan & Cui (2005). This discrepancy may indicate that the jet in FR Is are systematically stronger than in general LLAGNs.

We thank Wei Cui, Luis Ho, and Rodrigo Nemmen for their valuable comments, and D. Donato for providing us with his observational data. This work is supported by the One-Hundred-Talent Program of China, the National Science Fund for Distinguished Young Scholars (grant 10325314), and the NSFC (grants number 10333020, 10543002, and 10543003).

## REFERENCES

- Andernach, H., et al. 1992, A&AS, 93, 331
- Balmaverde, B., Capetti, A., & Grandi, P. 2006, A&A, 451, 35
- Bicknell, G. V. 1995, ApJS, 101, 29
- Blandford, R. D., & Begelman, M. C. 1999, MNRAS, 301, L1

- Blandford, R. D., & Znajek, R. L. 1977, MNRAS, 179, 433
- Bondi, M., et al. 2000, MNRAS, 314, 11
- Bower, G. A., et al. 2000, ApJ, 534, 189
- Bridle, A. H., et al. 1979, ApJ, 228, 9
- Cao, X. W., & Rawlings, S. 2004, MNRAS, 349, 1419
- Canvin, J. R., et al. 2005, MNRAS, 363, 1223
- Capetti, A., et al. 2002, A&A, 383, 104
- Celotti, A., Ghisellini, G., & Chiaberge, M. 2001, MNRAS, 321, 1
- Chiaberge, M., et al. 2006, ApJ, 651, 728
- Chiaberge, M., et al. 2005, ApJ, 625, 716
- Chiaberge, M., et al. 2002, ApJ, 571, 247
- Chiaberge, M., Capetti, A., & Celotti, A. 1999, A&A, 349, 77
- Corbel, S., et al. 2003, A&A, 400, 1007
- Cotton, W. D., et al. 1995, ApJ, 452, 605
- Donato, D., Sambruna, R. M., & Gliozzi, M. 2004, ApJ, 617, 915
- Evans, D. A., et al. 2006, ApJ, 642, 96
- Fabian, A. C., & Rees, M. J. 1995, MNRAS, 277, 55
- Fabbiano, G., et al. 2004, ApJ, 616, 730
- Fabbiano, G., et al. 2003, ApJ, 588, 175
- Falcke, H., Körding, E., & Markoff, S. 2004, A&A, 414, 895
- Fanaroff B. L., & Riley J. M. 1974, MNRAS, 167, 31
- Fender, R. P., Gallo, E., & Jonker, P. G. 2003, MNRAS, 343, 99
- Feretti, L., et al. 1999, A&A, 341, 29
- Gallo, E., et al. 2006, MNRAS, 370, 1351



- Gallo, E., Fender, R. P., & Pooley, G. G. 2003, MNRAS, 344, 60
- Garcia, M. R., et al. 2005, ApJ, 632, 1042
- Giovannini, G., et al. 2005, ApJ, 618, 635
- Giovannini, G., et al. 2001, ApJ, 552, 508
- Giovannini, G., et al. 1988, A&A, 199, 73
- Giozzi, M., Sambruna, R. M., & Brandt, W. N. 2003, A&A, 408, 949
- Gopal-Krishna, & Wiita, P. J. 2000, A&A, 363, 507
- Hardcastle, M. J., et al. 2002, MNRAS, 334, 182
- Hardcastle, M. J., et al. 2001, MNRAS, 326, 1499
- Hardcastle, M. J., & Worrall, D. M. 1999, MNRAS, 309, 969
- Hawley, J. F., & Balbus, S. A. 2002, ApJ, 573, 738
- Heinz, S. 2004, MNRAS, 355, 835
- Ho, L. C. 2005, Ap&SS, 300, 219
- Ho, L. C., Terashima, Y., & Ulvestad 2003, ApJ, 589, 783
- Igumenshchev, I. V., Narayan, R., & Abramowicz, M. A. 2003, ApJ, 592, 1042
- Jones, D. L., Terzian, Y., & Sramek, R. A. 1981, ApJ, 246, 28
- Kato, S., Fukue, J., & Mineshige, S. 1998, Black-hole accretion disks (Kyoto: Kyoto Univ. Press)
- Katz-Stone, D. M., & Rudnick, L. 1997, ApJ, 488, 146
- Körding, E., Falcke, H., & Corbel, S. 2006, A&A, 456, 439
- Kuulkers, E. 1998, NewAR, 42, 1
- Laing, R. A., & Bridle, A. H. 2002, MNRAS, 336, 328
- Laing, R. A., et al. 1999, MNRAS, 306, 513
- Laing, R. A., & Bridle, A. H. 1987, MNRAS, 228, 557

- Leahy, J. P., Pooley, G. G., & Jagers, W. J. 1986, *A&A*, 156, 234
- Leeuw, L. L., Sansom, A. E., & Robson, E. I. 2000, *MNRAS*, 311, 683
- Marchesini, D. et al. 2004, *MNRAS*, 351, 733
- Macchetto F., et al. 1991, *ApJ*, 373, 55
- Markoff, S. et al. 2005, *ApJ*, 635, 1203
- Markoff, S. et al. 2003, *A&A*, 397, 645
- Martel, A. R., et al. 1999, *ApJS*, 122, 81
- Martel, A. R., et al. 2000, *ApJS*, 130, 267
- Merloni, A., et al. 2006, *New Astronomy*, 11, 567
- Merloni, A., Heinz, S., & di Matteo, T. 2003, *MNRAS*, 345, 1057
- Narayan, R. 2005, *Ap&SS*, 300, 177
- Narayan, R. 2002, in *Lighthouses of the Universe*, eds. M. Gilfanov, R. Sunyaev, & E. Churazov (Berlin: Springer), 405
- Narayan, R., Igumenshchev, I. V., & Abramowicz, M. A. 2000, *ApJ*, 539, 798
- Narayan, R., Mahadevan, R., & Quataert, E. 1998, in *Theory of Black Hole Accretion Disks*, eds. by M. A. Abramowicz, G. Bjornsson, and J. E. Pringle. (Cambridge University Press), 148
- Narayan, R., & Yi, I. 1995, *ApJ*, 444, 231
- Narayan, R., & Yi, I. 1994, *ApJ*, 428, L13
- Nemmen, R. S., et al. 2006, *ApJ*, 643, 652
- Parma, P. et al. 2003, *A&A*, 397, 127
- Pellegrini, S. 2005, *ApJ*, 624, 155
- Pellegrini, S., et al. 2007, Submitted to *ApJ*(astro-ph/0701642)
- Pellegrini, S. 2003, *ApJ*, 585, 677
- Piran, T. 1999, *PhR*, 314, 575

- Ptak, A., et al. 2004, ApJ, 606, 173
- Quataert, E., & Gruzinov, A. 2000, ApJ, 539, 809
- Quataert, E., et al. 1999, ApJ, 525, L89
- Quillen, A. C., Almog, J., & Yukita, M. 2003, ApJ, 126, 2677
- Reynolds, C. S.; Garofalo, D., Begelman, M. C. 2006, ApJ, 651, 1023
- Reynolds, C. S., et al. 1996a, MNRAS, 283, 111
- Reynolds, C. S., et al. 1996b, MNRAS, 283, 873
- Rodriguez et al. 2007, ApJ, in press (astro-ph/0611341)
- Soria, R., et al. 2006, ApJ, 640, 143
- Spada, M., et al. 2001, MNRAS, 325, 1559
- Spencer, R. C., et al. 1991, MNRAS, 250, 225
- Stone, J. M., Pringle, J. E., & Begelman, M. C. 1999, MNRAS, 310, 1002
- Tansley, D., et al. 2000, MNRAS, 317, 623
- Trussoni, E., et al. 2003, A&A, 403, 889
- Venturi, T., Dallacasa, D., Stefanachi, F. 2004, A&A, 422, 515
- Venturi, T., et al. 2000, A&A, 363, 84
- Verdoes Kleijn, G. A., et al. 2002, AJ, 123, 1334
- Wang, R., Wu, X.-B., Kong, M.-Z. 2006, ApJ, 645, 890
- Worrall, D. M., & Birkinshaw, M. 2005, MNRAS, 360, 926
- Worrall, D. M., et al. 2003, MNRAS, 343, 73
- Worrall, D. M., et al. 2001, MNRAS, 326, 7
- Wu, Q. W., & Cao, X. W. 2005, ApJ, 621, 130
- Xu, C., et al. 2000, AJ, 120, 2950
- Xue, Y. Q. & Cui, W. 2007, A&A, in press

- Yuan, F., 2007, conference proceedings to appear in “The Central Engine of Active Galactic Nuclei”, ed. L. C. Ho and J.-M. Wang (astro-ph/0701638)
- Yuan, F., Shen, Z.-Q., & Huang, L. 2006, ApJ, 642, 45
- Yuan, F., Cui, W. & Narayan, R. 2005, ApJ, 620, 905
- Yuan, F., & Cui, W. 2005, ApJ, 629, 408
- Yuan, F., & Narayan, R. 2004, ApJ, 612, 724
- Yuan, F., Quataert, E., & Narayan, R. 2003, ApJ, 598, 301
- Yuan, F., et al. 2002, A&A, 391, 139

Table 1. Points used in Spectral Energy Distributions

Filter	$\log_{10}(\nu)$	$\log_{10}(\nu L_\nu)$	Resolution <sup>a</sup>	Ref.
3C 346				
1.7 GHz	9.23	41.26	$\sim 1\text{mas}$	C95
5 GHz	9.70	41.90	$\sim 1''$	G88
8 GHz	9.92	42.13	$\sim 1\text{ mas}$	C95
F702W	14.63	43.14	$\sim 0.1''$	C99
B2 0755 + 37				
1.7 GHz	9.23	40.03	$\sim 1''$	W01
5 GHz	9.70	40.72	$\sim 1''$	C02
F702W	14.63	42.04	$\sim 0.1''$	C02
3C 31				
1.7 GHz	9.23	38.75	$\sim 5\text{ mas}$	X00
5 GHz	9.70	39.46	$\sim 1\text{ mas}$	G01
8.6 GHz	9.93	39.70	$\sim 1''$	H02
345 GHz	11.53	41.22	$\sim 50''$	Q03
F555W	14.57	40.86	$\sim 0.1''$	K02
F814W	14.73	40.85	$\sim 0.1''$	K02
3C 317				
1.7 GHz	9.23	40.19	$\sim 1\text{ mas}$	V00
5 GHz	9.70	40.73	$\sim 1\text{ mas}$	V00
F210M	15.13	40.46	$\sim 0.1''$	C02
F702W	14.63	41.37	$\sim 0.1''$	C02
F160W	14.27	41.79	$\sim 0.1''$	T03
B2 0055 + 30				
5 GHz	9.70	40.26	$\sim 1''$	G05
F814	14.57	41.18	$\sim 0.1''$	C02
3C 66B				
1.7 GHz	9.23	39.43	$\sim 5\text{ mas}$	X00
5 GHz	9.70	39.97	$\sim 1\text{ mas}$	G01
345 GHz	11.54	41.50	$\sim 50''$	Q03
LW1	13.82	42.54	$\sim 1''$	Q03
LW2	13.32	42.33	$\sim 1''$	Q03
LW3	13.40	42.54	$\sim 1''$	Q03
F814W	14.57	41.60	$\sim 0.1''$	C02
3C 449				
1.5 GHz	9.17	38.26	$\sim 1''$	S97
5 GHz	9.70	39.08	$\sim 1''$	S97
8.3 GHz	9.92	39.37	$\sim 1''$	S97
F702W	14.63	40.82	$\sim 0.1''$	C02
3C 272.1				

Table 1—Continued

Filter	$\log_{10}(\nu)$	$\log_{10}(\nu L_\nu)$	Resolution <sup>a</sup>	Ref.
1.7 GHz	9.23	37.72	$\sim 1$ mas	J81
5 GHz	9.70	38.30	$\sim 1''$	G88
8.1 GHz	9.90	38.48	$\sim 1$ mas	J81
146 GHz	11.17	39.64	$\sim 10''$	L00
221 GHz	11.34	39.82	$\sim 10''$	L00
345 GHz	11.53	39.96	$\sim 10''$	Q03
350 GHz	11.54	40.10	$\sim 10''$	L00
677 GHz	11.82	40.16	$\sim 10''$	L00
LW3	13.32	40.31	$\sim 1''$	Q03
LW7	13.49	40.57	$\sim 1''$	Q03
LW2	13.65	40.94	$\sim 1''$	Q03
L	13.93	40.53	$\sim 1''$	Q03
F205W	14.16	40.05	$\sim 0.1''$	B00
F160W	14.27	40.16	$\sim 0.1''$	B00
F110W	14.43	40.11	$\sim 0.1''$	B00
F814W	14.57	40.00	$\sim 0.1''$	C02
F547W	14.73	39.98	$\sim 0.1''$	B00

Note. — The F110W, F160W, F205W filters refer to those from NICMOS (on board *HST*)  $1 - 2\mu\text{m}$ . F547W, F702W, F814W filters refer to optical WFPC2/*HST* measurements. The LW1, LW2, LW3, LW7 filters refer to  $4 - 15\mu\text{m}$  data from ISOCAM images. L band measurements are based on ground based images obtained at the Infrared Telescope Facility (IRTF, Quillen et al. (2003)).

References. — X00 VLBA (Xu et al. 2000); G01 VLBI (Giovannini et al. 2001); H02 VLA (Hardcastle et al. 2002); Q03 ISO and IRTF (Quillen et al. 2003); K02 HST (Verdoes Kleijn et al. 2002); V00 VLBI (Venturi et al. 2000); C95 VLBI Cotton et al. (1995); C99 HST (Chiaberge et al. 1999); C02 HST (Capetti et al. 2002); G88 VLA (Giovannini et al. 1988); G05 VLA (Giovannini et al. 2005); S97 VLA (Katz-Stone & Rudnick 1997); C02 HST (Capetti et al. 2002); T03 HST (Trussoni et al. 2003) L00 SCUBA (Leeuw et al. 2000); B00 HST (Bower et al. 2000); J81 VLBI (Jones et al. 1981); W01 VLA (Worrall et al. 2001);

<sup>a</sup>The resolution of different telescopes which are listed in references. The ‘mas’ means milli-arcsecond.

Table 2. Accretion and jet properties

Source	Redshift	Angle(deg) <sup>a</sup>	log10 $M_{\text{BH}}^{\text{b}}$	$L_X/L_{\text{Edd}}^{\text{c}}$	$\dot{m}_{\text{jet}}$	$\dot{m}(10R_{\text{S}})$	$ratio^{\text{d}}(\%)$	$\dot{m}(R_{\text{B}})^{\text{e}}$	$\dot{m}_B^{\text{f}}$	$L_{\text{Kin}}/\dot{M}(10R_{\text{S}})c^2$
3C 346	0.1620	30	8.89	$1.8 \times 10^{-4}$	$3.5 \times 10^{-5}$	$4.4 \times 10^{-3}$	0.91	$2.8 \times 10^{-2}$	$3.1 \times 10^{-3}$	0.03
B2 0755+37	0.0428	34	8.93	$5.2 \times 10^{-6}$	$1.75 \times 10^{-5}$	$< 4.5 \times 10^{-4}$	$> 3.9$	$< 8.9 \times 10^{-3}$	$3.2 \times 10^{-2}$	$> 0.10$
3C 31	0.0170	52	7.89	$4.4 \times 10^{-6}$	$2.7 \times 10^{-5}$	$3.0 \times 10^{-4}$	9.0	$3.7 \times 10^{-3}$	$2.1 \times 10^{-4}$	0.19
3C 317	0.0345	50	8.80	$3.4 \times 10^{-6}$	$1.7 \times 10^{-5}$	$1.9 \times 10^{-4}$	8.9	$4.7 \times 10^{-3}$	$4.5 \times 10^{-3}$	0.28
B2 0055+30	0.0165	35	9.18	$2.4 \times 10^{-6}$	$7.0 \times 10^{-6}$	$2.0 \times 10^{-4}$	3.5	$2.7 \times 10^{-3}$	$1.4 \times 10^{-2}$	0.08
3C 66B	0.0213	45	8.84	$1.0 \times 10^{-6}$	$1.0 \times 10^{-5}$	$< 1.7 \times 10^{-4}$	$> 5.9$	$< 2.6 \times 10^{-3}$	$2.5 \times 10^{-2}$	$> 0.18$
3C 449	0.0171	80	8.42	$8.0 \times 10^{-7}$	$2.0 \times 10^{-5}$	$1.4 \times 10^{-4}$	14.3	$1.9 \times 10^{-3}$	$1.7 \times 10^{-5}$	0.44
3C 272.1	0.0035	63	8.35	$8.3 \times 10^{-8}$	$4.9 \times 10^{-6}$	$< 6.7 \times 10^{-5}$	$> 7.3$	$< 1.9 \times 10^{-3}$	$6.0 \times 10^{-2}$	$> 0.22$

<sup>a</sup>inclination angle of the jet with an uncertainty of several degrees.

<sup>b</sup>in unit of  $M_{\odot}$ , which is derived from the correlation between the stellar velocity dispersion of the host bulge and its B band magnitude(Marchesini et al. 2004).

<sup>c</sup> $L_X$  is the X-ray luminosity in 2-10 keV band.

<sup>d</sup>ratio is  $\dot{m}_{\text{jet}}/\dot{m}(10 R_{\text{S}})$ .

<sup>e</sup> $\dot{m}(R_{\text{B}})$  is the dimensionless accretion rate at the Bondi radius through our spectra fitting.

<sup>f</sup> $\dot{m}_B$  is the dimensionless Bondi accretion rate estimated from the X-ray observation.

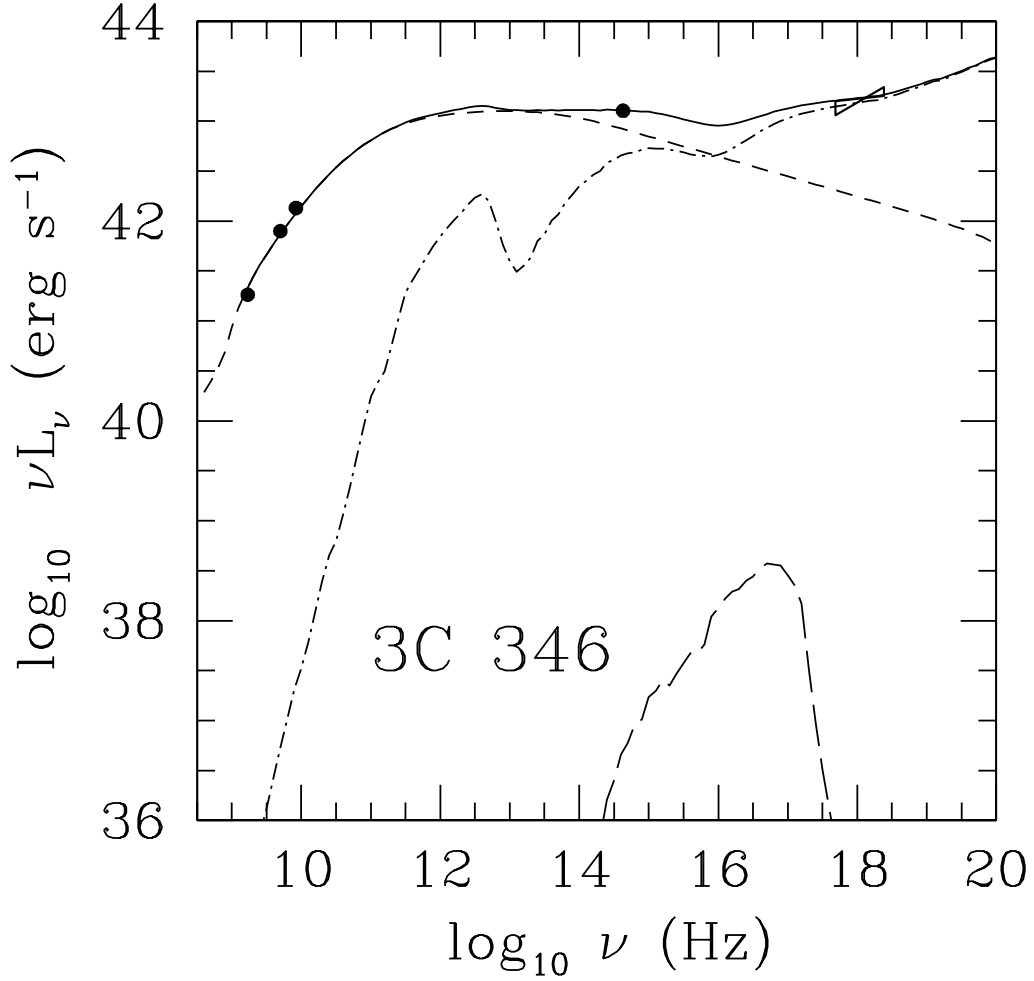


Fig. 1.— Spectral modeling results using the ADAF-jet model for 3C 346. The X-ray luminosity of this source is  $L_X = 1.8 \times 10^{-4} L_{\text{Edd}}$ . The dot-dashed, dashed, and the solid lines show the emissions from the ADAF, jet, and their sum, respectively. The thin long-dashed line is synchrotron-self-Compton spectrum of the jet. For this source, the X-ray emission is dominated by the ADAF rather than the jet.



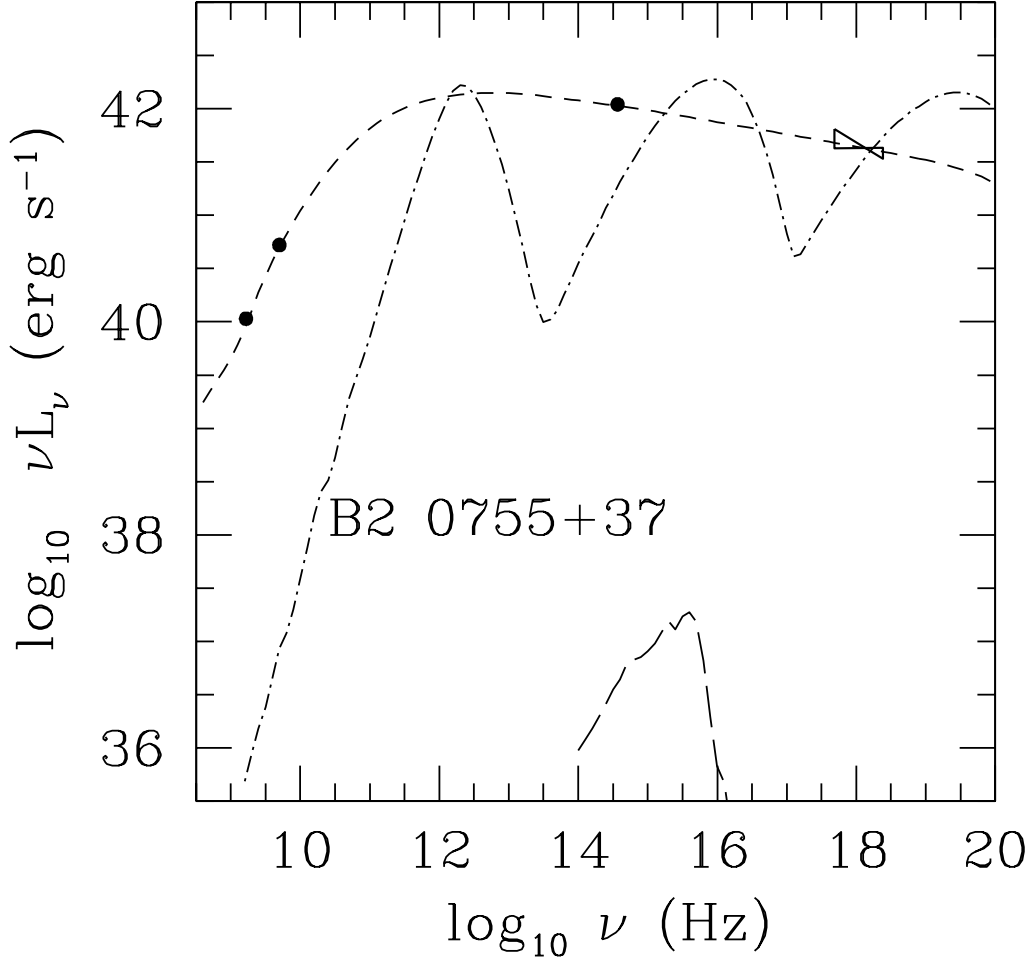


Fig. 2.— Spectral modeling results for B2 0755+37 ( $L_X = 5.2 \times 10^{-6} L_{\text{Edd}}$ ). The dashed line shows the emissions from the jet, it explains the X-ray spectrum very well. Also shown in the figure is the synchrotron-self-Compton spectrum of the jet (long-dashed line) and the spectrum produced by an ADAF model (dot-dashed line). The parameters of the ADAF are chosen so that it can produce a "correct" X-ray flux. Obviously the ADAF model cannot explain the X-ray spectrum since the spectrum it predicts is too hard.

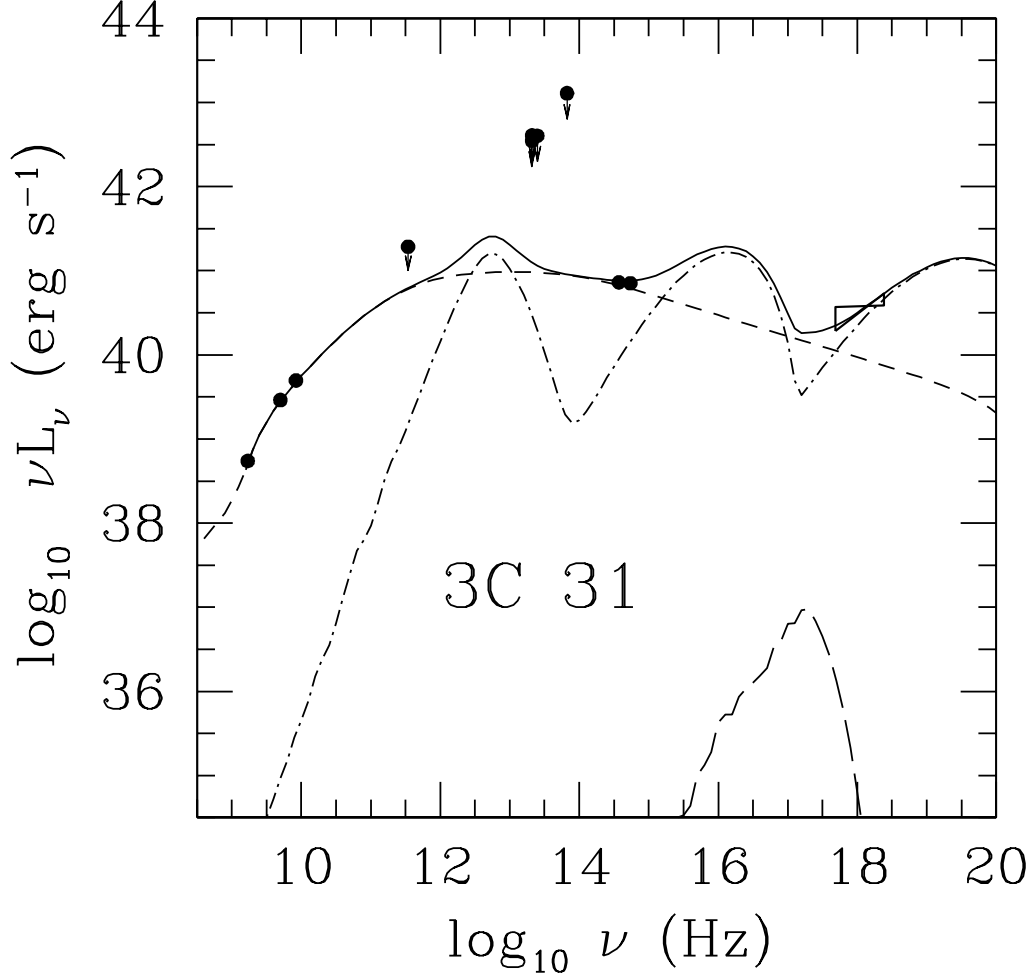


Fig. 3.— Spectral modeling results for 3C 31 ( $L_X = 4.4 \times 10^{-6} L_{\text{Edd}}$ ). The dot-dashed, dashed, and the solid lines show the emissions from the ADAF, jet, and their sum, respectively. The long-dashed line is synchrotron-self-Compton spectrum of the jet. For this source, the contributions from the ADAF and the jet are comparable.

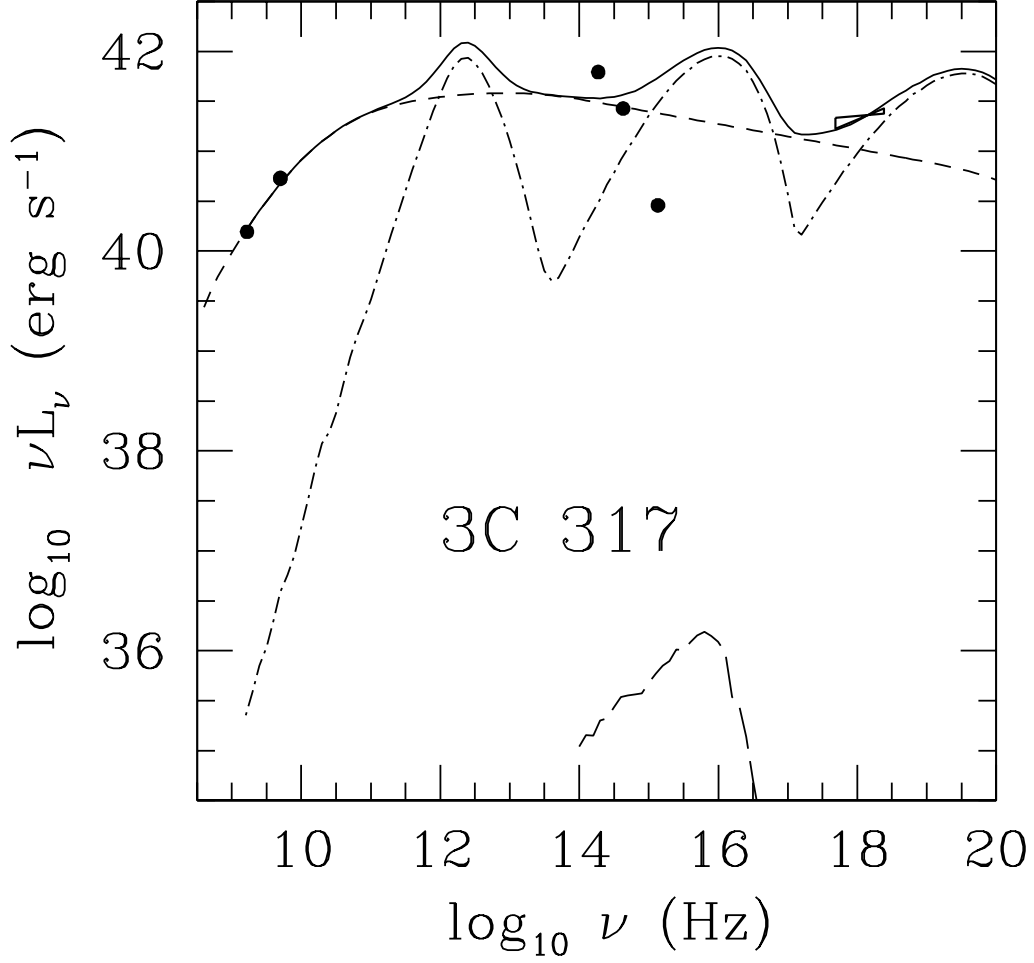


Fig. 4.— Spectral modeling results for 3C 317 ( $L_X = 3.4 \times 10^{-6} L_{\text{Edd}}$ ). The dot-dashed, dashed, and the solid lines show the emissions from the ADAF, jet, and their sum, respectively. The long-dashed line is synchrotron-self-Compton spectrum of the jet. For this source, the contributions from the ADAF and the jet are comparable.

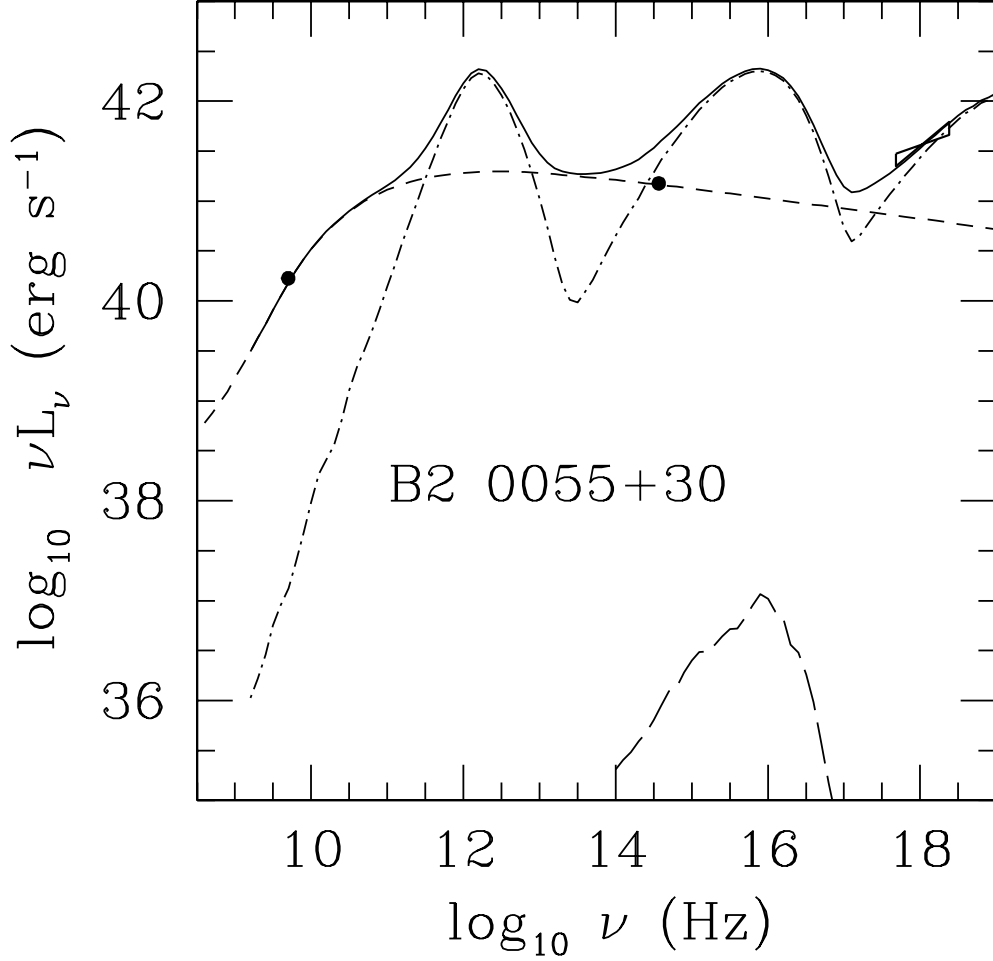


Fig. 5.— Spectral modeling results for B2 0055+30 ( $L_X = 2.4 \times 10^{-6} L_{\text{Edd}}$ ). The dot-dashed, dashed, and the solid lines show the emissions from the ADAF, jet, and their sum, respectively. The long-dashed line is synchrotron-self-Compton spectrum of the jet. The X-ray emission in this source is dominated by the ADAF, and the jet contributes a small fraction in soft X-ray band.

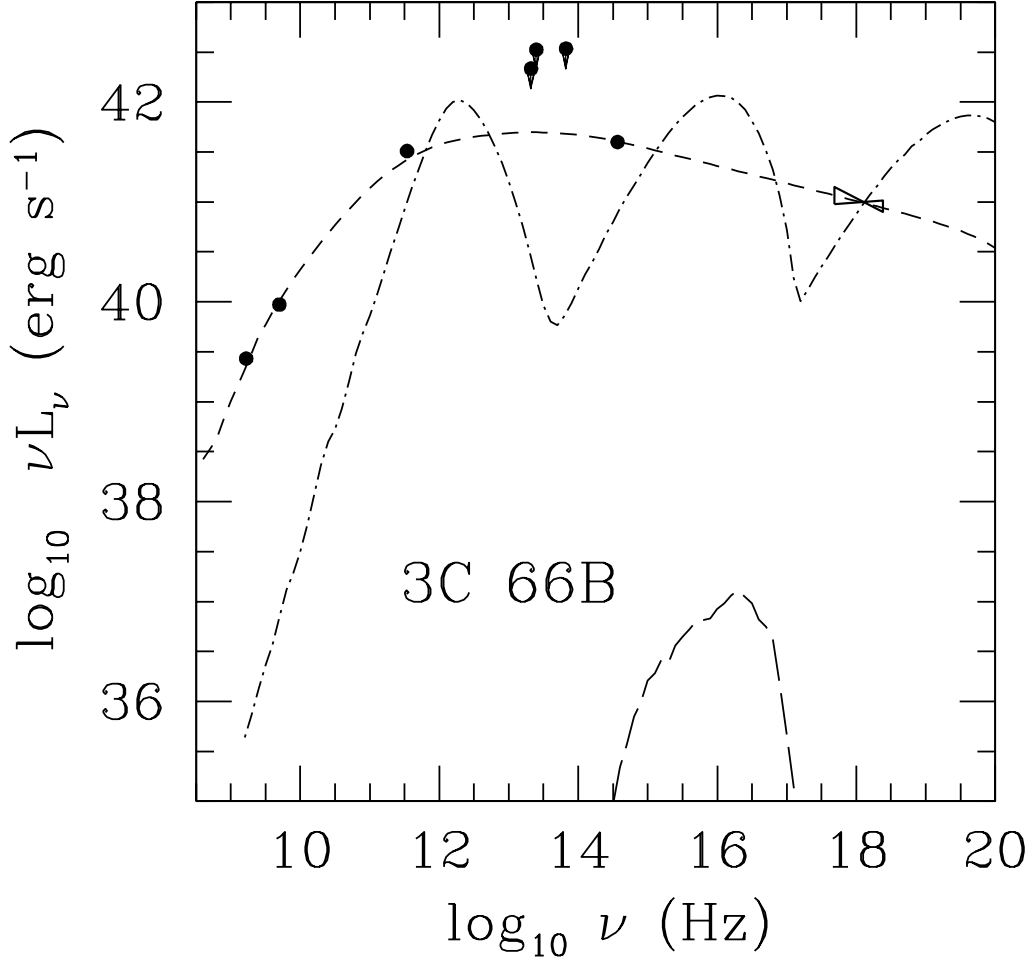


Fig. 6.— Spectral modeling results for 3C 66B ( $L_X = 1.0 \times 10^{-6} L_{\text{Edd}}$ ). The dashed line shows the emissions from the jet, it explains the X-ray spectrum very well. Also shown in the figure is the synchrotron-self-Compton spectrum of the jet (long-dashed line) and the spectrum produced by an ADAF model (dot-dashed line). The parameters of the ADAF are chosen so that it can produce a "correct" X-ray flux. Obviously the ADAF model cannot explain the X-ray spectrum since the spectrum it predicts is too hard.

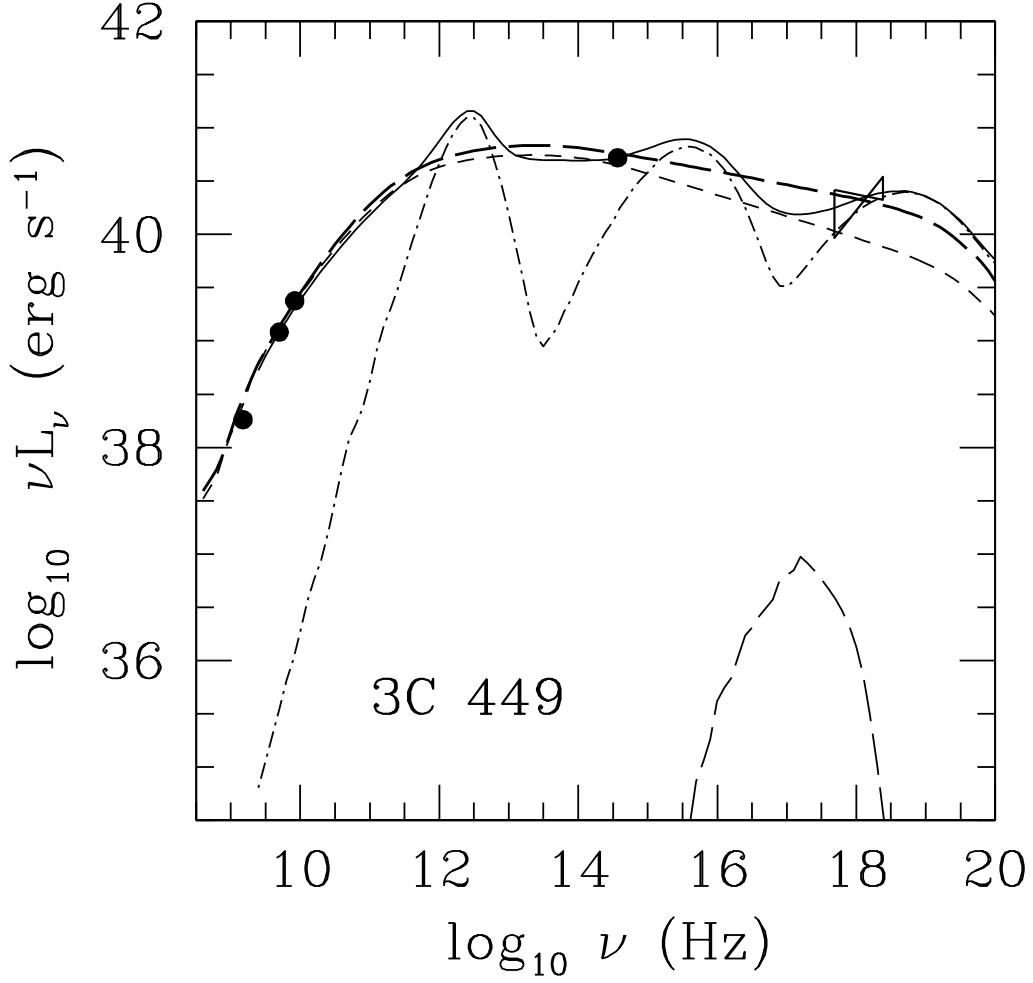


Fig. 7.— Spectral modeling results for 3C 449 ( $L_X = 8.0 \times 10^{-7} L_{\text{Edd}}$ ). The dot-dashed, thin short-dashed, and the solid lines show the emissions from the ADAF, jet, and their sum, respectively. The solid lines can well fit the X-ray spectrum. For this source, due to the relatively large error bar, the X-ray spectrum can also be fit by a pure jet model, as shown by the thick long-dashed line.

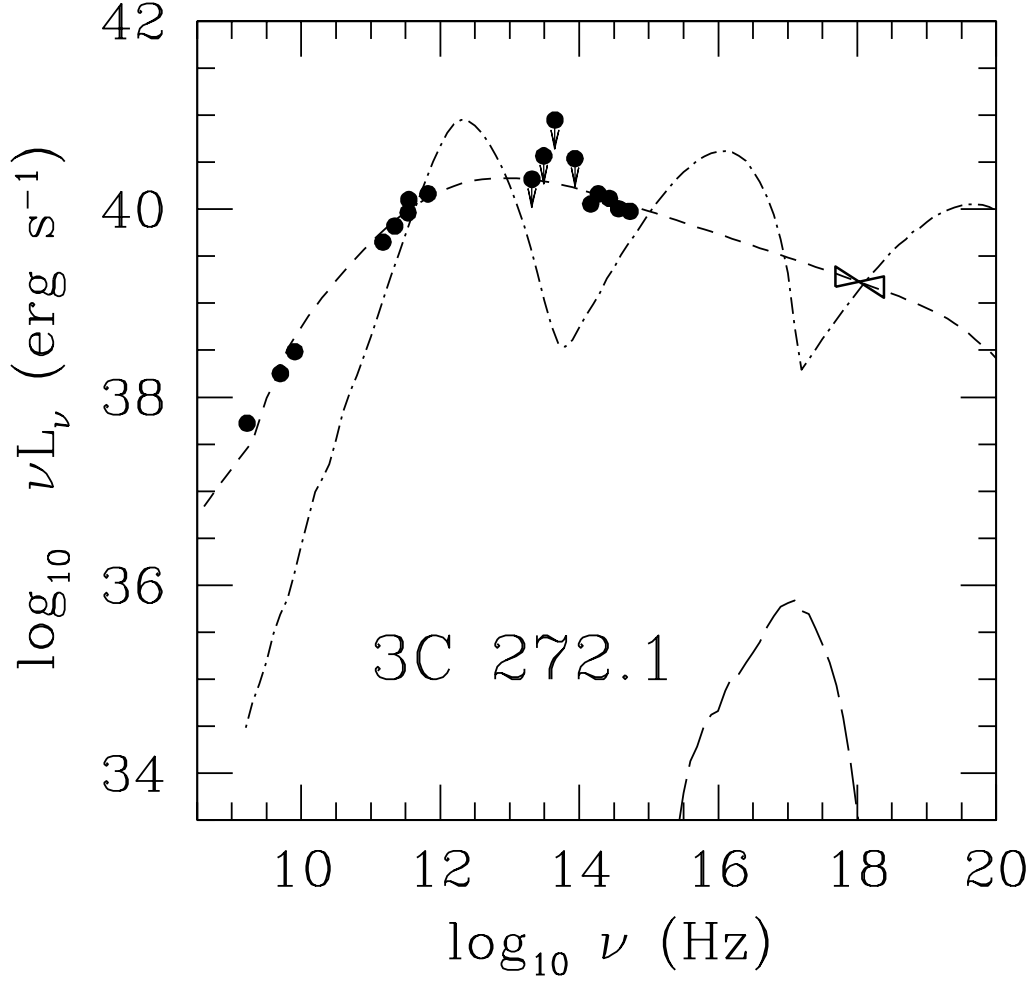


Fig. 8.— Spectral modeling results for 3C 272.1 ( $L_X = 6.8 \times 10^{-8} L_{\text{Edd}}$ ). The dashed line shows the emissions from the jet, it explains the X-ray spectrum very well. Also shown in the figure is the synchrotron-self-Compton spectrum of the jet (long-dashed line) and the spectrum produced by an ADAF model (dot-dashed line). The parameters of the ADAF are chosen so that it can produce a "correct" X-ray flux. Obviously the ADAF model cannot explain the X-ray spectrum since the spectrum it predicts is too hard.